Newcomer insulin secretory granules as a highly calcium-sensitive pool

Morten Gram Pedersen[a,1] and Arthur Sherman[b]

[a]Department of Information Engineering, University of Padua, I-35131 Padua, Italy; and [b]Laboratory of Biological Modeling, National Institute of Diabetes, Digestive, and Kidney Diseases, National Institutes of Health, Bethesda, MD 20892

Edited by Charles S. Peskin, New York University, and approved March 12, 2009 (received for review February 3, 2009)

Insulin secretion is biphasic in response to a step in glucose stimulation. Recent experiments suggest that 2 different mechanisms operate during the 2 phases, with transient first-phase secretion due to exocytosis of docked granules but the second sustained phase due largely to newcomer granules. Another line of research has shown that there exist 2 pools of releasable granules with different Ca^{2+} sensitivities. An immediately releasable pool (IRP) is located in the vicinity of Ca^{2+} channels, whereas a highly Ca^{2+}-sensitive pool (HCSP) resides mainly away from Ca^{2+} channels. We extend a previous model of exocytosis and insulin release by adding an HCSP and show that the inclusion of this pool naturally leads to insulin secretion mainly from newcomer granules during the second phase of secretion. We show that the model is compatible with data from single cells on the HCSP and from stimulation of islets by glucose, including L- and R-type Ca^{2+} channel knockouts, as well as from Syntaxin-1A-deficient cells. We also use the model to investigate the relative contribution of calcium signaling and pool depletion in controlling biphasic secretion.

β-cells | biphasic secretion | exocytosis | pancreatic islets | vesicles

Insulin is secreted from pancreatic β-cells in response mainly to raised plasma glucose concentration. Metabolism of the sugar leads to an increased ATP-to-ADP ratio as well as other metabolic second messengers. The change in nucleotide concentrations closes ATP-sensitive potassium channels, which triggers oscillatory electrical activity and calcium influx through voltage gated calcium channels. The resulting elevation in the intracellular Ca^{2+} concentration induces exocytosis of insulin-containing granules and release of the hormone. Besides this triggering pathway, the amount of released insulin is also controlled by a less-well-understood amplifying pathway (1).

When stimulated by a step of glucose or potassium, insulin is secreted in a characteristic biphasic pattern with a large peak lasting ≈5 min, followed by a second phase with a flat or slowly rising rate of secretion, depending on the conditions (2–4). Because the loss of first phase secretion is an early marker of diabetes (5, 6), a defect that appears to have its origin on the level of single islets (7), understanding biphasic insulin release is of physiological importance.

There is evidence that first-phase secretion is due to granules already residing at the membrane, whereas an enhanced supply of new vesicles to the plasma membrane is responsible for the second phase (2). Secretion can rise during the second phase, whereas calcium on average remains constant. Calcium then may determine the probability per vesicle of release, whereas the enhanced resupply increases the number of vesicles available for calcium near the plasma membrane to work on. Resupply in this view is an element in the amplifying pathway because it increases the effectiveness of calcium (8, 9). Knockout studies have shown that L-type Ca^{2+} channels control first-phase secretion (10), whereas other types, such as R-type channels, are important for the second phase (11). Classically it has been thought that newly arrived vesicles must go through a sequence of steps, docking and priming, before fusing (12), but more recent data suggest that newcomers fuse with only a short delay during the second phase (13–15).

Most immediate exocytosis occurs with a very low affinity for Ca^{2+}, showing an EC_{50} value of tens of micromolar (16). Such high concentrations are only attained right below the calcium channels in so-called microdomains (17, 18). Thus, at least the immediately releasable pool (IRP) of granule must be situated in the vicinity of calcium channels. Indeed, there is strong evidence for direct physical coupling between some of the granules immediately available for release and L-type channels (19, 16).

In addition to the fast microdomain controlled exocytosis, another highly calcium-sensitive pool (HCSP) of granules has been described with an EC_{50} value of a few micromolar (20, 21). This pool is not a subset of the granules residing within microdomains because it is not exhausted by short depolarizations. A similar pool exists in chromaffin cells (22) and in rod photoreceptors (23). The difference in calcium affinity between the IRP and the HCSP might be explained by different Ca^{2+} sensors regulating the 2 pools (24). The calcium-sensing proteins involved in exocytosis in β-cells appear to be synaptotagmins (Syts), in particular the isoforms Syt7 and Syt9 (25). Synaptotagmin-7 has a Ca^{2+} affinity on the order of a few micromolar (26), whereas Syt9 has a much lower affinity (27), even lower than the Syt1 isoform (28), which has an affinity of tens of micromolar (26). Another candidate is Syt3 (29), although its role in primary β-cells is controversial (25). Syt3 is a high-affinity sensor with Ca^{2+}-sensing properties similar to Syt7 (26).

The molecular machinery controlling docking and fusion of insulin-containing granules shares with the release of neurotransmitters and other hormones a central role for SNARE proteins (12, 24, 30,). Besides participating in SNARE complexes, syntaxin (Synt) is also involved in docking of granules. Synt1A knockout mice have a reduced number of docked granules (14), a fact that is in line with studies in chromaffin cells (31) and with the findings that interaction between Munc18–1, granuphilin and Syntaxin-1 is involved in docking of granules in insulin-secreting cells (32, 33), and that the Munc18–1–Syntaxin-1 complex is crucial for docking of granules in chromaffin cells (34–36).

Interestingly, although granuphilin (15, 32) and Synt1A (14) knockout cells show a reduced number of docked granules, they do secrete insulin, suggesting that docking is not a prerequisite for fusion, as also suggested in other cell types (37, 38). Synt1A- and granuphilin-deficient animals show virtually no first phase of insulin secretion, and almost all fusion events are due to new-

Author contributions: M.G.P. and A.S. designed research, performed research, and wrote the paper.

The authors declare no conflict of interest.

This article is a PNAS Direct Submission.

[1]To whom correspondence should be addressed at: Department of Information Engineering, University of Padua, Via Gradenigo 6/A, I-35131 Padua, Italy. E-mail: pedersen@dei.unipd.it.

This article contains supporting information online at www.pnas.org/cgi/content/full/0901202106/DCSupplemental.

comers (14, 15). In addition, first-phase secretion from wild-type cells has been found to occur mainly from previously docked granules at Synt1A-rich locations, whereas second-phase secretion is mainly due to newcomer granules fusing away from Synt1A clusters (14). Because syntaxin-1 and L-type Ca^{2+} channels colocalize (39), the results of Ohara-Imaizumi et al. (14) show that first-phase secretion takes place mostly at L-type Ca^{2+} channels, whereas second-phase fusion events occur away from L-type channels, in accordance with Ca^{2+}-channel knockout experiments (10, 11).

We build on a previous model (9), which accounted for first- and second-phase secretion and reproduced Ca^{2+}-channel knockout experiments but did not consider the HCSP or newcomer granules. Because both HCSP granules and newcomers fuse away from L-type Ca^{2+} channels, we hypothesized that they might be overlapping sets of vesicles. Because newcomers are independent of docking proteins such as Syntaxin-1A and granuphilin, we propose further that granules that are still not completely docked to the cell membrane have a higher calcium sensitivity and therefore respond to bulk cytosolic calcium rather than the microdomain calcium that triggers exocytosis of the IRP (21, 20). Docking would lower the affinity for calcium, and attachment to L-type Ca^{2+} channels would become a prerequisite for fusion of docked granules. We show, by incorporating the HCSP in a previous model (9), that these assumptions have as a natural consequence that the second phase of secretion is mainly due to newcomer granules (13–15), which fuse before docking completely (14, 15). The model is found to be compatible with data from single cells on the HCSP and from stimulation of islets by glucose, including L- and R-type Ca^{2+}-channel knockouts. We also use the model to investigate the relative contribution of calcium signaling and pool depletion in controlling biphasic secretion.

Theory

Our model is modified from that of Chen et al. (9) as follows. Granules are assumed to mobilize to an ''almost-docked'' pool (12), tether to the membrane (35), dock, become primed and attach to L-type calcium channels. We have replaced the exocytosis cascade with a single fusion step, where the rate follows a sigmoidal relation with a low affinity for microdomain calcium (16). We have assumed that granules can also fuse with a high affinity for cytosolic Ca^{2+} after tethering but before docking completely. The pool of tethered granules is hence naturally identified with the HCSP (20, 21). An overview of the pools is given in Fig. 1.

Microdomain Ca^{2+} receives influx from L-type Ca^{2+} channels, whereas Ca^{2+} flux through R-type (and other non-L-type) channels enters the bulk cytosolic Ca^{2+}. We assume that L-type channels are responsible for 50% of the total Ca^{2+} currents (10). Microdomain and cytosolic Ca^{2+} are assumed to exchange by diffusion, and Ca^{2+} is extruded from the bulk cytosol.

In response to a step in the glucose concentration, β-cells in islets exhibit a typical pattern consisting of a first phase with intense electrical activity and a raised cytosolic Ca^{2+} concentration, followed by a second phase with bursting electrical activity and calcium oscillations (1). To simulate glucose stimulation, we approximated the oscillations with a square wave of membrane potential alternating between -70 mV and -20 mV and also increased the rate of mobilization from the reserve pool by a factor of 3. The period of the oscillations was either 1 min, to mimic fast bursting, or 6 min, to mimic slow oscillations, and the first depolarization was prolonged to varying degrees to assess the effects of first-phase depolarization duration. The fast HCSP protocol is described in the legend of Fig. 2.

Parameters were chosen so as to reproduce figure 4 of Barg et al. (40), figure 3 of Yang and Gillis (21) and figure 1*B* of Ohara-Imaizumi et al. (13) and to get pool sizes as reported by Rorsman and Renström (12). Parameters were changed based on proposed mechanisms and are described in the figure cap-

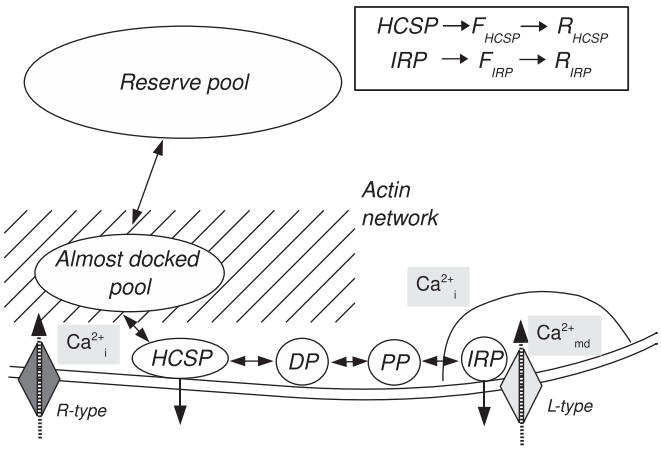

Fig. 1. A schematic overview of the model. Granules from the reserve pool, assumed to be infinite, approach the membrane through the actin network where they enter from the almost-docked pool. When reaching the membrane, they are assumed to tether weakly and fuse with high affinity for bulk cytosolic Ca^{2+} (Ca^{2+}_i). Hence, these granules are identified with the HCSP. Tethered granules can mature further by docking (DP, docked pool), undergo priming (PP, primed pool), and attach to L-type Ca^{2+} channels, thus entering the IRP. We identify the readily releasable pool (RRP) as the sum of IRP, PP, and DP. From the IRP, granules can fuse with low affinity for microdomain Ca^{2+} (Ca^{2+}_{md}). Fusion from both HCSP and IRP are assumed to follow a Hill function. (*Inset*) After fusion, the granules enter a ''fused pool'' (F_{HCSP} or F_{IRP}). The fusion pore can then expand, after which the granule belongs to a ''releasing pool'' (R_{HCSP} or R_{IRP}). The insulin secretion rate is defined as the release flux from the 2 releasing pools.

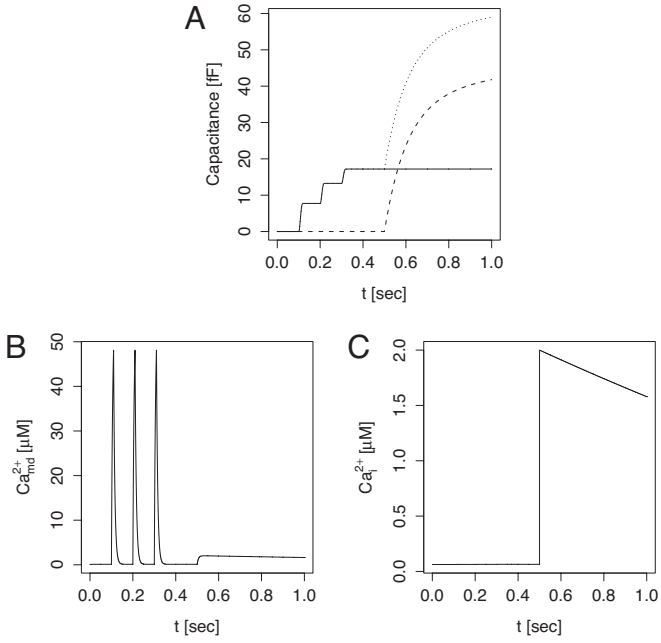

Fig. 2. Protocol as in figure 8 of Wan et al. (20) and figure 3 in Yang and Gillis (21). (*A*) The capacitance increases resulting from IRP (solid) and HCSP (dashed) and the total (dotted). (*B*)The membrane potential was held at -70 mV and then depolarized to $+20$ mV 3 times for 10 ms with 100-ms intervals, resulting in spikes in microdomain Ca^{2+}. (*C*) At t = 0.5 s, the cytosolic calcium concentration was raised to 2 μM to simulate flash release of Ca^{2+}.

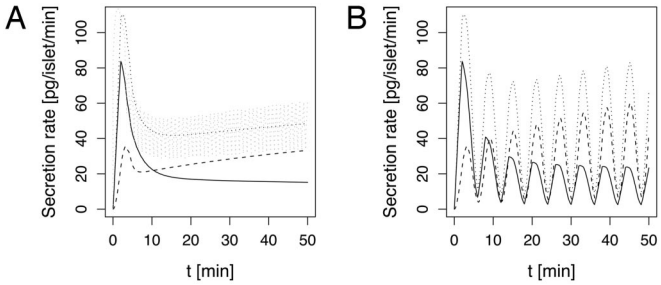

Fig. 3. Two-minute moving average of secretion rates from granules from the HCSP [newcomers (14), dashed], the IRP (full) and total secretion (dotted). (*A*) A fast burst-like pattern with a period of 1 min was imposed. The gray, dotted line shows the instantaneous secretion rate. (*B*) A slow burst-like pattern with a period of 6 min was imposed, resulting in pulsatile insulin secretion.

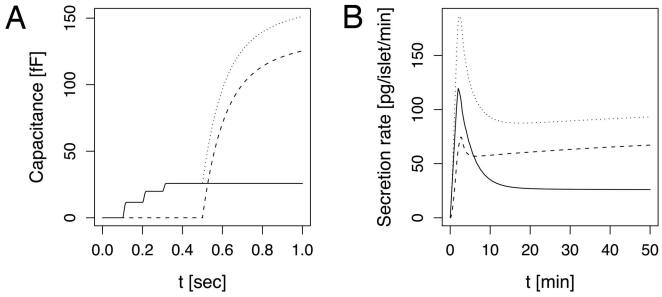

Fig. 4. Simulating the effect of PKC activation. Although the HCSP is enlarged much more than the RRP (*A*, compare with Fig. 2*A*), the insulin secretion profile during fast bursting is hardly modified because the first and second phases are enhanced to a similar degree (*B*, compare with Fig. 3*A*). The mobilization rate in *A* was enhanced 3-fold relative to Fig. 2*A* to represent the effect of PKC. In *B*, the rate before glucose stimulation was also increased 3-fold and then further increased to 5-fold over basal to represent the effect of glucose on mobilization (vs. the factor 3 used in Fig. 3*A*). The docking rate r_3 was decreased 50% to simulate stabilization of the HCSP granules.

tions. After changing parameters, a prerun was done until steady-state was reached, and this state was then used as the initial condition.

All equations and parameters can be found in the supporting information (SI) *Text*. Simulations were done with the cvode solver of XPPAUT (41).

Results

In response to the combination of depolarizations and flash release of Ca^{2+} used by Wan et al. (20) and Yang and Gillis (21), our model reproduces satisfactorily the experimentally observed changes in membrane capacitance (Fig. 2). The depolarizations result in spikes in microdomain Ca^{2+} below the L-type channels, but have little effect on bulk cytosolic Ca^{2+}. Consequently, IRP granules fuse whereas there is no exocytosis from the HCSP. HCSP fusion occurs when cytosolic Ca^{2+} is raised to 2 μM, with no further release from the IRP.

In simulated responses to a glucose step, insulin release shows oscillations (Fig. 3). During the first phase, insulin secretion occurs mostly from the readily releasable pool (RRP), defined as the sum of the pools of docked, primed and immediately releasable granules, whereas the HCSP is mainly responsible for the second phase of insulin secretion. This is true for both fast and a slow burst-like patterns. Because the HCSP corresponds to vesicles that are assumed not to be completely docked, we identify these granules with newcomers, which fuse shortly after reaching the membrane (13–15).

When activating PKC with phorbol esters, Ca^{2+} sensitivity and fusion kinetics are unchanged, but both the HCSP and the RRP increase in size (20, 21). Whereas the RRP increases ≈50%, the HCSP increases 3- to 4-fold. Similar effects were found in chromaffin cells (22). The larger total number of releasable granules (HCSP plus RRP) suggests that the rate of recruitment to the membrane is increased. PKC is known to participate in remodeling of the actin network below the cell membrane in chromaffin cells (42), a crucial step controlling recruitment of granules from the reserve pool, including in β-cells (43). If there were no other effects on rates, this would lead to a proportional increase in size of the various pools in our model. We therefore hypothesized that, in addition to increasing the recruitment rate, PKC stabilizes the transient highly calcium-sensitive state by lowering the rate of complete docking. This allows a greater increase in the HCSP than in the RRP (Fig. 4*A*, compare with Fig. 2*A*). Because the HCSP is amplified more than the RRP, one might expect second-phase secretion to be enhanced much more than the first phase. However, in agreement with experiments by Kasai et al. (44), the biphasic secretion pattern did not change, apart from an overall amplification when we simulated glucose stimulation using the fast burst-like protocol (Fig. 4*B*). This is because the HCSP in the model contributes to the first peak of secretion as well as the second phase.

It has been suggested that biphasic insulin release could be a result not of vesicle kinetics but of the biphasic Ca^{2+} pattern (24, 45). To test this hypothesis, we simulated the burst-like protocol with varying lengths of the first phase of depolarization (Fig. S1). We found that for first phases <2 min, the maximum secretion rate increased with first-phase length. However, for longer first-phase stimulations, there was no further increase. For first phases <2 min, the peak in secretion rate could be attributed to the Ca^{2+} first phase, whereas for longer stimuli the peak resulted from emptying of the RRP. We note that Henquin et al. (4) found that insulin peaks before Ca^{2+} and that stimulation by high K^+ concentrations gives a sustained calcium signal but a peak of insulin secretion (46). It is therefore unlikely that biphasic insulin release is controlled solely by the phasic calcium concentration, although it may contribute.

Schulla et al. (10) investigated insulin release in mice lacking L-type Ca^{2+} channels. Ca^{2+} responses were similar to wild-type animals, probably because of up-regulation of non-L-type channels, but the insulin release pattern was markedly changed, with a much smaller first phase and a reduced second phase of secretion. When we set the L-type conductance to zero, but up-regulate the non-L-type channels to compensate, the model reproduces this behavior (Fig. S2*A*). Virtually all release is from the HCSP, i.e., from newcomers, because there are no longer microdomains below L-type channels.

In contrast, mice with no R-type channels (11) showed a reduced Ca^{2+} signal, indicating no compensation from other types of Ca^{2+} channels, but first-phase insulin secretion was only slightly reduced. Second-phase insulin secretion, in contrast, was markedly reduced. Our model reproduces both these observations (Fig. S2*B*), with a reduction in secretion from the HCSP due to lower cytosolic Ca^{2+} concentration. Because most first-phase secretion is controlled by L-type microdomain calcium, which is virtually unchanged by the R-type knockout, the first phase persists. Notably, the rate of refilling of the RRP is unchanged because we assumed no Ca^{2+} dependence. We thus provide an alternative to the explanation proposed in ref. 11 and simulated in ref. 9.

Knockout of Syntaxin-1A (14), yields a secretion pattern similar to that observed in L-type Ca^{2+}-channel knockout mice. We hypothesized that the effect of Synt1A knockout could be attributed to a lower docking rate, because Synt1A knockout cells show a significantly reduced number of docked granules

(14). This assumption has little effect on second-phase secretion but reduces the first phase of secretion in the model (Fig. S3*A*), because the RRP and IRP are much smaller, in agreement with ref. 47, and L-type microdomain release is consequently reduced. An alternative way to simulate a pattern similar to R-type Ca^{2+}-channel knockout mice is to reduce the fusion rate from the HCSP from 30 s^{-1} to 1 s^{-1}, representing loss of the HCSP Ca^{2+} sensor. The insulin pattern shows a clear first peak of insulin release, whereas second-phase secretion is much lower than in wild-type animals (Fig. S3*B*). This is because of the near abolition of secretion from the HCSP, as in the case of R-type Ca^{2+}-channel knockout (Fig. S2*B*) but now with no change in the Ca^{2+} concentration.

Discussion

We have proposed here that 2 recent and still poorly understood findings in the regulation of insulin secretion from β-cells are tightly connected. We showed that the inclusion of an HCSP located away from L-type Ca^{2+} channels (20, 21) naturally leads to insulin release mainly from newcomer granules during the second phase of biphasic secretion (13–15). Based on the observation that the granules residing in the HCSP and RRP have similar properties (21), we hypothesized that the HCSP reflected a highly calcium-sensitive transient state of granules, which might mature further to join the RRP and IRP if not released during a susceptible time window. This is compatible with the observation that the IRP and RRP show low Ca^{2+} affinity (16). This was included in the model by assuming that granules have a higher calcium sensitivity before docking completely to the membrane, which could reflect the "weakly tethered" granules observed in chromaffin cells (35). Interestingly, "strong tethering"/docking is syntaxin dependent in chromaffin cells (35, 31), which corresponds to the low number of docked vesicles observed in Synt1A knockout β-cells (14). The strongest experimental test of this crucial assumption, would be to look for the HCSP in syntaxin-deficient cells. We predict that the HCSP is intact, and possibly even enlarged, in such cells (Fig. S4*A*).

Newcomer granules are thus assumed to fuse before docking completely and away from L-type Ca^{2+} channels. This agrees with the observation that second-phase secretion from newcomers occurs away from syntaxin clusters (14), which are known to be colocated with Ca^{2+} channels (39).

We did not include the Ca^{2+} effects on mobilization that were part of the previous version of the model (9). Although cytosolic Ca^{2+} is important for several processes such as activation of key mobilization and actin modifying proteins, such as PKC-MARCKS (42), CaM kinase II (48), gelsolin (49), and myosin Va (50, 51), this was done to keep the model simple and show that the loss of second-phase secretion in R-type Ca^{2+}-channel knockout mice (11) can be explained, at least partly, by less fusion from the HCSP due to a lower cytosolic Ca^{2+} concentration.

The model with HCSP functions similarly to the previous version (9), although second-phase secretion was entirely because of release from the RRP, which only contributes partly to the second phase in the present model (Fig. 3). The critical role for the HCSP in second-phase secretion is reflected in the prediction that reduced bulk Ca^{2+} is sufficient to account for loss of second phase in the R-type channel knockout. Loss of the HCSP Ca^{2+} sensor is similarly predicted to result in selective loss of the second phase (Fig. S3*B*). However, an intact HCSP, although necessary in the present model, is not sufficient for a sustained second phase, which also requires increased resupply to avoid depleting the HCSP. In other words, second phase requires both increased probability of release, via a switch to more sensitive granules, and increased vesicle number.

Although our argument is fundamentally kinetic, molecular bases for the processes assumed in the model are needed. Most central are the molecular events responsible for the change from a highly Ca^{2+} sensitive to a low-affinity state. One candidate for the HCSP Ca^{2+} sensor is synaptotagmin 7 (Syt7), which has higher Ca^{2+} sensitivity than Syt9 and Syt1 (26, 27). However, Syt7 knockout mice show reductions in both first- and second-phase insulin secretion (52), not the selective reduction in second phase predicted by the model for loss of the HCSP sensor. (Fig. S3*B*). Moreover, in chromaffin cells, Syt7 deletion does not alter exocytosis in the low-micromolar range (53). Another candidate for the HCSP Ca^{2+} sensor is the Syt3 isoform, which shows Ca^{2+} affinity similar to Syt7 (26). Syt3 has indeed been suggested to play a role in insulin secretion at low Ca^{2+} concentrations (29), although conflicting results have been reported in the literature (25).

The identification of the HCSP with newcomers and RRP with previously resident vesicles suggests that the HCSP is a transient state that follows partial docking and precedes full docking and priming. A candidate molecule to regulate the balance between the HCSP and the RRP is complexin. Such a role is supported by recent findings (54–56), which suggest that complexin stabilizes full SNARE complex formation, preventing nontriggered fusion by raising the concentration of calcium required for release and reducing the rate of back transition to the HCSP. This would have the effect of reducing release in the short run but of increasing potential release in response to a large increase of Ca^{2+} influx. Complexin might thus play an important role in low-stimuli situations such as fasting, where insulin release should be kept at a minimum, whereas refilling of the RRP prepares the swift response to any rapid change in plasma glucose concentration.

To model the effects of PKC activation, which enhances the size of the HCSP more than that of the RRP, we assumed that PKC stimulates recruitment of granules from the reserve pool and, in addition, stabilizes the HCSP by reducing the rate of complete docking. It has been suggested that SNAP-25 phosphorylation is largely responsible for the effects of PKC activation (57–59). Accordingly, the HCSP is increased more than the RRP by a phosphomimetic mutation of SNAP-25 (58, 59). Our assumption of PKC-enhanced mobilization is supported by the fact that SNAP-25 phosphorylation increases the rate of granule delivery (57), possibly because of SNAP-25–actin interactions (60), or more speculatively, because of a requirement for SNAP-25 in the weak tethering process described by Toonen et al. (35). Moreover, PKC is well known to have effects on the submembrane actin barrier because of activation of proteins involved in the remodeling of the actin network such as MARCKS (42). Such actin remodeling allows granules to arrive at the cell membrane and is important for second-phase insulin secretion (24, 43, 60). The assumption of HCSP stabilization is most easily explained by changed properties of SNAP-25 because of phosphorylation, which might reduce the rate of complete SNARE complex formation and hence full docking. PKC-mediated phosphorylation of SNAP-25 has been shown to increase SNAP-25–syntaxin binding (58), likely resulting in slower SNAP-25–syntaxin dissassembly, which has been suggested to interfere with complete SNARE complex formation, because a syntaxin molecule needs to be replaced by synaptobrevin for formation of the ternary complex (57). Enhanced SNAP-25–syntaxin binding might also hinder full docking of new granules at the IRP release sites, as has been suggested in the blind-drunk mouse, which has a mutation of SNAP-25b that leads to stabilization of the SNARE complex (24, 61). SNAP-25 phosphorylation and increased SNAP-25–syntaxin binding may thus account for our hypothesis of decreased full docking rate after PKC activation.

ACKNOWLEDGMENTS. M.G.P. was supported by the Lundbeck Foundation. A.S. was supported by the intramural research program of the National Institutes of Health, National Institute of Diabetes, Digestive, and Kidney Diseases.

1. Henquin J-C (2000) Triggering and amplifying pathways of regulation of insulin secretion by glucose. *Diabetes* 49:1751–1760.
2. Curry DL, Bennett LL, Grodsky GM (1968) Dynamics of insulin secretion by the perfused rat pancreas. *Endocrinology* 83:572–584.
3. Cerasi E, Luft R (1963) Plasma-insulin response to sustained hyperglycemia induced by glucose infusion in human subjects. *Lancet* 2:1359–1361.
4. Henquin J-C, Nenquin M, Stiernet P, Ahren B (2006) In vivo and in vitro glucose-induced biphasic insulin secretion in the mouse: Pattern and role of cytoplasmic Ca^{2+} and amplification signals in beta-cells. *Diabetes* 55:441–451.
5. Del Prato S, Marchetti P, Bonadonna RC (2002) Phasic insulin release and metabolic regulation in type 2 diabetes. *Diabetes* 51 Suppl 1:S109–S116.
6. Gerich JE (2002) Is reduced first-phase insulin release the earliest detectable abnormality in individuals destined to develop type 2 diabetes? *Diabetes* 51 Suppl 1:S117–S121.
7. Del Guerra S, et al. (2005) Functional and molecular defects of pancreatic islets in human type 2 diabetes. *Diabetes* 54:727–735.
8. Straub S, Shanmugam G, Sharp G (2004) Stimulation of insulin release by glucose is associated with an increase in the number of docked granules in the β-cells of rat pancreatic islets. *Diabetes* 53:3179–3183.
9. Chen Y, Wang S, Sherman A (2008) Identifying the targets of the amplifying pathway for insulin secretion in pancreatic beta-cells by kinetic modeling of granule exocytosis. *Biophys J* 95:2226–2241.
10. Schulla V, et al. (2003) Impaired insulin secretion and glucose tolerance in beta cell-selective Ca(v)1.2 Ca^{2+} channel null mice. *EMBO J* 22:3844–3854.
11. Jing X, et al. (2005) CaV2.3 calcium channels control second-phase insulin release. *J Clin Invest* 115:146–154.
12. Rorsman P, Renström E (2003) Insulin granule dynamics in pancreatic beta cells. *Diabetologia* 46:1029–1045.
13. Ohara-Imaizumi M, et al. (2004) TIRF imaging of docking and fusion of single insulin granule motion in primary rat pancreatic beta-cells: Different behaviour of granule motion between normal and Goto–Kakizaki diabetic rat beta-cells. *Biochem J* 381:13–18.
14. Ohara-Imaizumi M, et al. (2007) Imaging analysis reveals mechanistic differences between first- and second-phase insulin exocytosis. *J Cell Biol* 177:695–705.
15. Kasai K, Fujita T, Gomi H, Izumi T (2008) Docking is not a prerequisite but a temporal constraint for fusion of secretory granules. *Traffic* 9:1191–1203.
16. Barg S, et al. (2001) Fast exocytosis with few Ca^{2+} channels in insulin-secreting mouse pancreatic B cells. *Biophys J* 81:3308–3323.
17. Neher E (1998) Vesicle pools and Ca^{2+} microdomains: New tools for understanding their roles in neurotransmitter release. *Neuron* 20:389–399.
18. Rutter GA, Tsuboi T, Ravier MA (2006) Ca^{2+} microdomains and the control of insulin secretion. *Cell Calcium* 40:539–551.
19. Wiser O, et al. (1999) The voltage sensitive Lc-type Ca^{2+} channel is functionally coupled to the exocytotic machinery. *Proc Natl Acad Sci USA* 96:248–253.
20. Wan Q-F, et al. (2004) Protein kinase activation increases insulin secretion by sensitizing the secretory machinery to Ca^{2+}. *J Gen Physiol* 124:653–662.
21. Yang Y, Gillis KD (2004) A highly Ca^{2+}-sensitive pool of granules is regulated by glucose and protein kinases in insulin-secreting INS-1 cells. *J Gen Physiol* 124:641–651.
22. Yang Y, Udayasankar S, Dunning J, Chen P, Gillis KD (2002) A highly Ca^{2+}-sensitive pool of vesicles is regulated by protein kinase C in adrenal chromaffin cells. *Proc Natl Acad Sci USA* 99:17060–17065.
23. Thoreson WB, Rabl K, Townes-Anderson E, Heidelberger R (2004) A highly Ca^{2+}-sensitive pool of vesicles contributes to linearity at the rod photoreceptor ribbon synapse. *Neuron* 42:595–605.
24. Eliasson L, et al. (2008) Novel aspects of the molecular mechanisms controlling insulin secretion. *J Physiol* 586:3313–3324.
25. Gauthier BR, Wollheim CB (2008) Synaptotagmins bind calcium to release insulin. *Am J Physiol Endocrinol Metab* 295:1279–1286.
26. Sugita S, Shin O-H, Han W, Lao Y, Südhof TC (2002) Synaptotagmins form a hierarchy of exocytotic Ca^{2+} sensors with distinct Ca^{2+} affinities. *EMBO J* 21:270–280.
27. Shin O-H, Maximov A, Lim BK, Rizo J, Südhof TC (2004) Unexpected Ca^{2+}-binding properties of synaptotagmin 9. *Proc Natl Acad Sci USA* 101:2554–2559.
28. Xu J, Mashimo T, Südhof TC (2007) Synaptotagmin-1, -2, and -9: Ca^{2+} sensors for fast release that specify distinct presynaptic properties in subsets of neurons. *Neuron* 54:567–581.
29. Brown H, et al. (2000) Synaptotagmin III isoform is compartmentalized in pancreatic beta-cells and has a functional role in exocytosis. *Diabetes* 49:383–391.
30. Lang J (1999) Molecular mechanisms and regulation of insulin exocytosis as a paradigm of endocrine secretion. *Eur J Biochem* 259:3–17.
31. de Wit H, Cornelisse LN, Toonen RFG, Verhage M (2006) Docking of secretory vesicles is syntaxin dependent. *PLoS ONE* 1:e126.
32. Gomi H, Mizutani S, Kasai K, Itohara S, Izumi T (2005) Granuphilin molecularly docks insulin granules to the fusion machinery. *J Cell Biol* 171:99–109.
33. Tomas A, Meda P, Regazzi R, Pessin JE, Halban PA (2008) Munc 18–1 and granuphilin collaborate during insulin granule exocytosis. *Traffic* 9:813–832.
34. Voets T, et al. (2001) Munc18–1 promotes large dense-core vesicle docking. *Neuron* 31:581–591.
35. Toonen RF, et al. (2006) Dissecting docking and tethering of secretory vesicles at the target membrane. *EMBO J* 25:3725–3737.
36. Gerber SH, et al. (2008) Conformational switch of syntaxin-1 controls synaptic vesicle fusion. *Science* 321:1507–1510.
37. Szule JA, et al. (2003) Calcium-triggered membrane fusion proceeds independently of specific presynaptic proteins. *J Biol Chem* 278:24251–24254.
38. Edmonds BW, Gregory FD, Schweizer FE (2004) Evidence that fast exocytosis can be predominantly mediated by vesicles not docked at active zones in frog saccular hair cells. *J Physiol* 560:439–450.
39. Yang SN, et al. (1999) Syntaxin 1 interacts with the L(D) subtype of voltage-gated Ca^{2+} channels in pancreatic beta cells. *Proc Natl Acad Sci USA* 96:10164–10169.
40. Barg S, et al. (2002) Delay between fusion pore opening and peptide release from large dense-core vesicles in neuroendocrine cells. *Neuron* 33:287–299.
41. Ermentrout G (2002) *Simulating, Analyzing, and Animating Dynamical Systems: A Guide to XPPAUT for Researchers and Students* (SIAM Books, Philadelphia).
42. Trifaró J-M, Gasman S, Gutiérrez LM (2008) Cytoskeletal control of vesicle transport and exocytosis in chromaffin cells. *Acta Physiol* 192:165–172.
43. Wang Z, Oh E, Thurmond DC (2007) Glucose-stimulated Cdc42 signaling is essential for the second phase of insulin secretion. *J Biol Chem* 282:9536–9546.
44. Kasai K, et al. (2005) Rab27a mediates the tight docking of insulin granules onto the plasma membrane during glucose stimulation. *J Clin Invest* 115:388–396.
45. Meissner HP (1976) Electrical characteristics of the beta-cells in pancreatic islets. *J Physiol* 72:757–767.
46. Henquin J-C, Ishiyama N, Nenquin M, Ravier MA, Jonas J-C (2002) Signals and pools underlying biphasic insulin secretion. *Diabetes* 51 Suppl 1:S60–S67.
47. Vikman J, Ma X, Hockerman GH, Rorsman P, Eliasson L (2006) Antibody inhibition of synaptosomal protein of 25 kDa (SNAP-25) and syntaxin 1 reduces rapid exocytosis in insulin-secreting cells. *J Mol Endocrinol* 36:503–515.
48. Gromada J, et al. (1999) CaM kinase II-dependent mobilization of secretory granules underlies acetylcholine-induced stimulation of exocytosis in mouse pancreatic B-cells. *J Physiol* 518(Pt 3):745–759.
49. Tomas A, Yermen B, Min L, Pessin JE, Halban PA (2006) Regulation of pancreatic beta-cell insulin secretion by actin cytoskeleton remodelling: Role of gelsolin and cooperation with the MAPK signalling pathway. *J Cell Sci* 119:2156–2167.
50. Ivarsson R, Jing X, Waselle L, Regazzi R, Renström E (2005) Myosin 5a controls insulin granule recruitment during late-phase secretion. *Traffic* 6:1027–1035.
51. Varadi A, Tsuboi T, Rutter GA (2005) Myosin Va transports dense core secretory vesicles in pancreatic MIN6 beta-cells. *Mol Biol Cell* 16:2670–2680.
52. Gustavsson N, et al. (2008) Impaired insulin secretion and glucose intolerance in synaptotagmin-7 null mutant mice. *Proc Natl Acad Sci USA* 105:3992–3997.
53. Schonn J-S, Maximov A, Lao Y, Südhof TC, Sørensen JB (2008) Synaptotagmin-1 and -7 are functionally overlapping Ca^{2+} sensors for exocytosis in adrenal chromaffin cells. *Proc Natl Acad Sci USA* 105:3998–4003.
54. Cai H, et al. (2008) Complexin II plays a positive role in Ca^{2+}-triggered exocytosis by facilitating vesicle priming. *Proc Natl Acad Sci USA* 105:19538–19543.
55. Brose B (2008) For better or for worse: Complexins regulate SNARE function and vesicle fusion. *Traffic* 9:1403–1413.
56. Südhof TC, Rothman JE (2009) Membrane fusion: Grappling with SNARE and SM proteins. *Science* 323:474–477.
57. Nagy G, et al. (2002) Protein kinase C-dependent phosphorylation of synaptosome-associated protein of 25 kDa at Ser187 potentiates vesicle recruitment. *J Neurosci* 22:9278–9286.
58. Yang Y, et al. (2007) Phosphomimetic mutation of Ser-187 of SNAP-25 increases both syntaxin binding and highly Ca^{2+}-sensitive exocytosis. *J Gen Physiol* 129:233–244.
59. Shu Y, Liu X, Yang Y, Takahashi M, Gillis KD (2008) Phosphorylation of SNAP-25 at Ser187 mediates enhancement of exocytosis by a phorbol ester in INS-1 cells. *J Neurosci* 28:21–30.
60. Thurmond DC, Gonelle-Gispert C, Furukawa M, Halban PA, Pessin JE (2003) Glucose-stimulated insulin secretion is coupled to the interaction of actin with the t-SNARE (target membrane soluble *N*-ethylmaleimide-sensitive factor attachment protein receptor protein) complex. *Mol Endocrinol* 17:732–742.
61. Jeans AF, et al. (2007) A dominant mutation in Snap25 causes impaired vesicle trafficking, sensorimotor gating, and ataxia in the blind-drunk mouse. *Proc Natl Acad Sci USA* 104:2431–2436.

Supporting Information

Pedersen et al. 10.1073/pnas.0901202106

SI Text

Equations. Granule compartments measured in number of granules. Abbreviations as in Fig. 1 except AP, "almost-docked pool;" FIP, F_{IRP}; RIP, R_{IRP}; FHP, F_{HCSP}; and RHP, R_{HCSP}.

$$IRP' = r_1\,PP - r_{-1}\,IRP - f_I(C_{md})IRP, \quad [1]$$

$$PP' = r_{-1}\,IRP - (r_1 + r_{-2})PP + r_2\,DP, \quad [2]$$

$$DP' = r_3\,HCSP + r_{-2}\,PP - (r_{-3} + r_2)DP, \quad [3]$$

$$HCSP' = r_4\,AP - (r_{-4} + r_3)HCSP + r_{-3}\,DP - f_H(C_i)HCSP, \quad [4]$$

$$AP' = r_5 - (r_{-5} + r_4)\,AP + r_{-4}\,HCSP, \quad [5]$$

$$FIP' = f_I(C_{md})IRP - u_2\,FIP, \quad [6]$$

$$RIP' = u_2\,FIP - u_3\,RIP, \quad [7]$$

$$FHP' = f_H(C_i)HCSP - u_2\,FHP, \quad [8]$$

$$RHP' = u_2 FHP - u_3 RHP. \quad [9]$$

Fusion rates from IRP (f_I) and HCSP (f_H) follow Hill functions.

$$f_I(C_{md}) = f_{I,\max}\frac{C_{md}^n}{C_{md}^n + K_I^n}, \quad f_H(C_i) = f_{H,\max}\frac{C_i^n}{C_i^n + K_H^n}, \quad [10]$$

where C_{md} is the Ca^{2+} concentration in microdomains, C_i the bulk cytosolic Ca^{2+} concentration, measured in micromolar.

Calcium compartments are modeled as in Chen et al. (9) and described by

$$C'_{md} = -f_{md}J_L - f_{md}B(C_{md} - C_i), \quad [11]$$

$$C'_i = -f_i\,J_R + f_v f_i B(C_m d - C_i) - f_i\,L. \quad [12]$$

Molar fluxes through L- and R-type channels:

$$J_L = \alpha I_L/v_{md}, \qquad J_R = \alpha I_R/v_{cell}. \quad [13]$$

where the respective currents are

$$I_L = g_L m_\infty(V)(V - V_{Ca}), \qquad I_R = g_R m_\infty(V)(V - V_{Ca}), \quad [14]$$

with $m_\infty(v) = 1/(1 + \exp((V_m - V)/s_m))$.

Calcium pumps and stores

$$J_{serca} = J_{serca,\max}\frac{C_i^2}{K_{serca}^2 + C_i^2}, \; J_{pmca} = J_{pmca,\max}\frac{C_i}{K_{pmca} + C_i}, \quad [15]$$

$$J_{ncx} = J_{ncx,0}(C_i - 0.25\mu M),\; L = J_{serca} + J_{pmca} + J_{ncx} + J_{leak}. \quad [16]$$

To follow capacitance increases, the fusion fluxes are multiplied by 3.5 fF per granule and integrated, i.e.,

$$Cap_{IRP} = 3.5\int_0^t f_I\,IRP, \quad Cap_{HCSP} = 3.5\int_0^t f_H\,HCSP. \quad [17]$$

Similarly, to follow secretion, the release fluxes are multiplied by 9 pg per granule per islet (see ref. 1) and by 60 to change from seconds to minutes.

$$Secr_{IRP} = 60 \cdot 9 \cdot u_3 RI, \quad Secr_{HCSP} = 60 \cdot 9 \cdot u_3 RH. \quad [18]$$

We show mainly the 2-min moving averages of these expression.

Initial Conditions. All simulations are started from steady-state. For the standard parameters (see below) this yields the following initial conditions: IRP(0) = 7.69, PP(0) = 38.45, DP(0) = 297.17, HCSP(0) = 12.06, AP(0) = 964.8, FIP(0) = 1.5×10^{-7}, RIP(0) = 2.3×10^{-5}, FHP(0) = 8×10^{-5}, RHP(0) = 0.012, $C_{md}(0)$ = 0.0674 μM, $C_i(0)$ = 0.06274 μM.

Parameters. Vesicle dynamics parameters (s^{-1}): $r_1 = 0.005$, $r_{-1} = 0.025$, $r_2 = 0.00014$, $r_{-2} = 0.001$, $r_3 = 0.00185$, $r_{-3} = 0.00007$, $r_4 = 0.002$, $r_{-4} = 0.16$, $r_5 = 0.22$, $r_{-5} = 0.0002$, $u_1 = 2000$, $u_2 = 3$, $u_3 = 0.02$.

Fusion constants: $f_{I,\max} = 30\ s^{-1}$, $K_I = 22\ \mu M$, $f_{H,\max} = 30\ s^{-1}$, $K_H = 2.5\ \mu M$, $n = 4$.

Calcium currents: $g_L = 150$ pS, $g_R = 150$ pS, $V_m = -20$ mV, $V_{Ca} = 25$ mV, $s_m = 5$ mV.

Calcium fluxes: $J_{serca,max} = 41\ \mu M/s$, $K_{serca} = 0.27\ \mu M$, $J_{pmca,max} = 2{,}141\ \mu M/s$, $K_{pmca} = 0.5\ \mu M$, $J_{leak} = -0.9441\ \mu M/s$, $J_{ncx,0} = 18.67\ s^{-1}$, $f_{md} = 0.01$, $f_i = 0.01$, $B = 17{,}250\ s^{-1}$, $\alpha = 5.18\ 10^{-15}\ \mu mol/s/fA$, $v_{cell} = 1.15$ pl, $v_{md} = 0.00385\ 10^{-3}$ pl, $f_v = v_{md}/v_{cell}$.

1. Chen Y, Wang S, Sherman A (2008) Identifying the targets of the amplifying pathway for insulin secretion in pancreatic beta-cells by kinetic modeling of granule exocytosis. *Biophys J* 95:2226–2241.

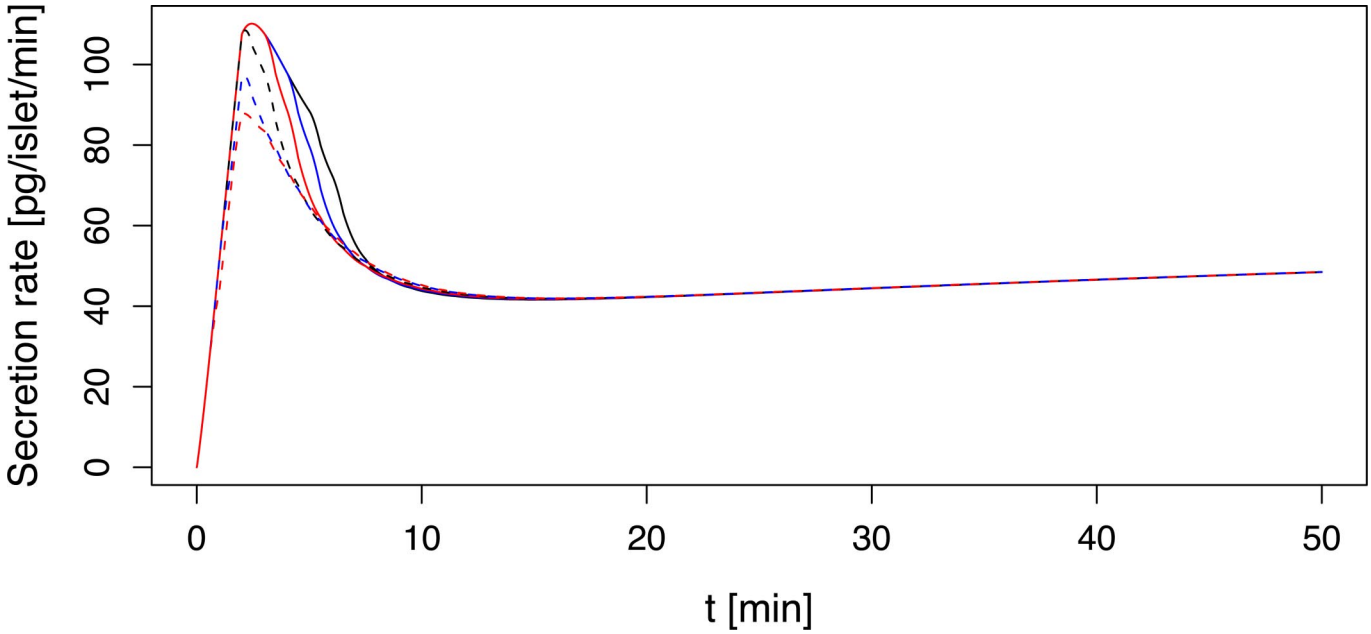

Fig. S1. Two-minute moving average of total secretion rates due to an imposed burst-like pattern with a period of 1 min. The length of the depolarization was varied from 30 s (dashed red), through 1 min (dashed blue), 2 min (dashed black), 3 min (solid red), 4 min (solid blue) to 5 min (solid black). (see ref. 1).

1. Henquin J-C, Nenquin M, Stiernet P, Ahren B (2006) In vivo and in vitro glucose-induced biphasic insulin secretion in the mouse: Pattern and role of cytoplasmic Ca^{2+} and amplification signals in beta-cells. *Diabetes* 55:441–451.

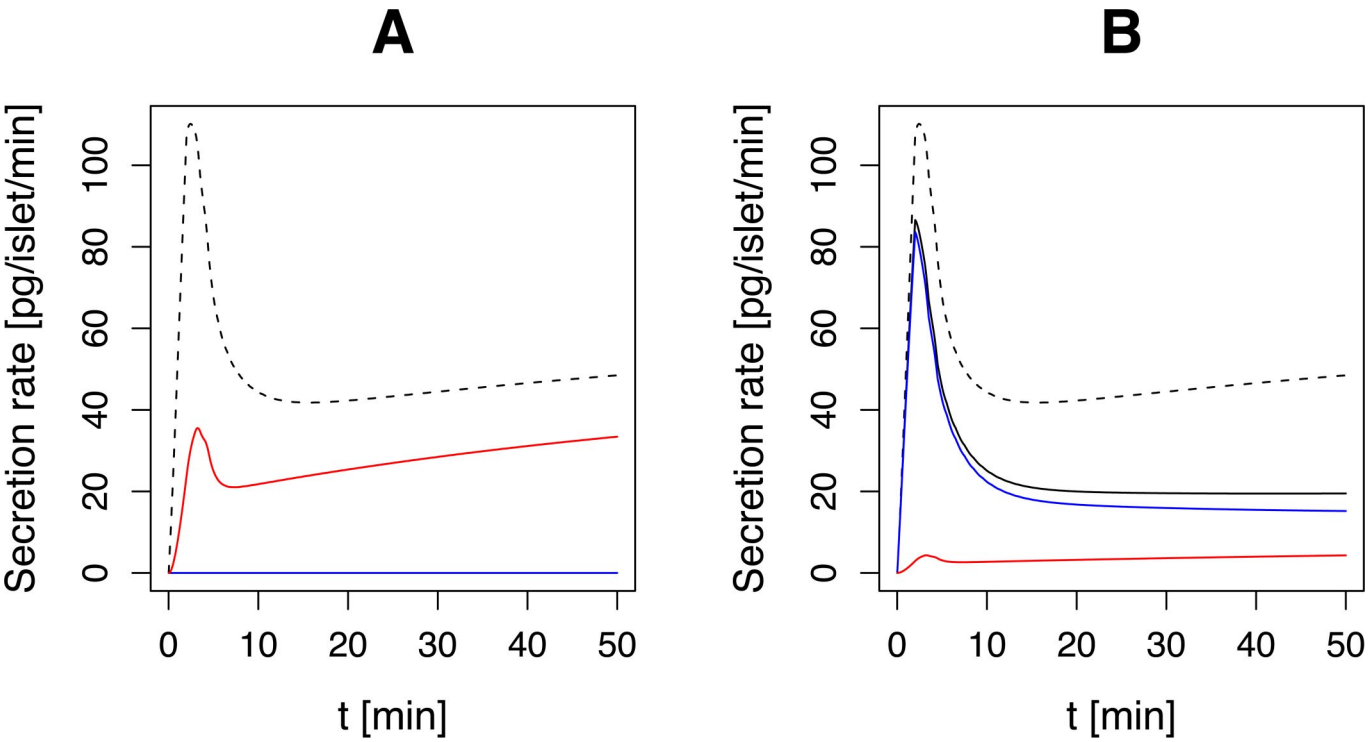

Fig. S2. Two-minute moving average of total secretion rates with an imposed burst-like pattern with a period of 1 min. (*A*) L-type knockout [g_L set to zero, and g_R = 300 pS up-regulated to compensate (1)]. (*B*) R-type knock-out (2) (g_R = 0 pS). Legends as in Fig. 3. For comparison, the dashed line taken from Fig. 3 shows total wild-type release.

1. Schulla V, et al. (2003) Impaired insulin secretion and glucose tolerance in beta cell-selective Ca(v)1.2 Ca^{2+} channel null mice. *EMBO J* 22:3844–3854.
2. Jing X, et al. (2005) CaV2.3 calcium channels control second-phase insulin release. *J Clin Invest* 115:146–154.

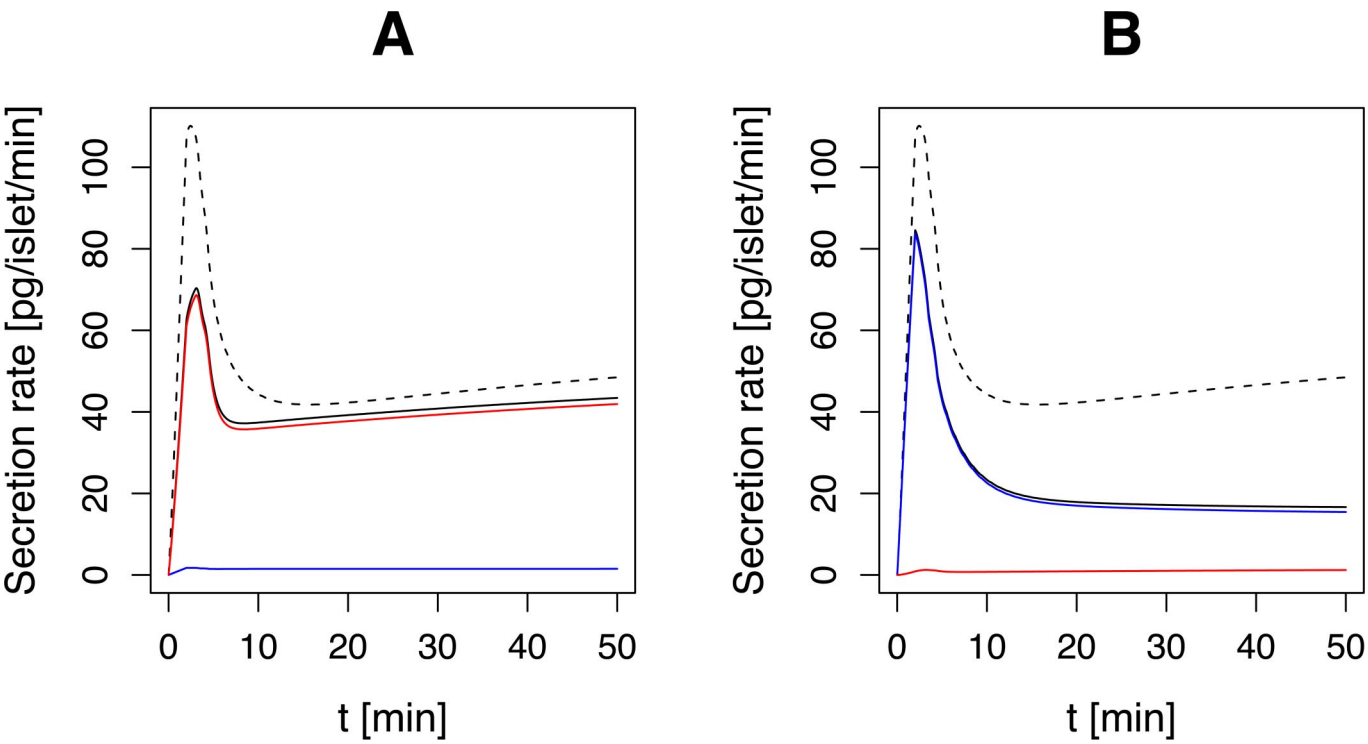

Fig. S3. Two-minute moving average of total secretion rates with an imposed burst-like pattern with a period of 1 min. (*A*) Synt1A knockout (low docking rate, r_3 reduced 90%) (1). (*B*) Hypothetical knockout of HCSP Ca^{2+} sensor (fusion from the HCSP lowered by a factor of 30). Legends as in Fig. 3. For comparison, the dashed line taken from Fig. 3 shows total wild-type release.

1. Ohara-Imaizumi M, et al. (2007) Imaging analysis reveals mechanistic differences between first- and second-phase insulin exocytosis. *J Cell Biol* 177:695–705.

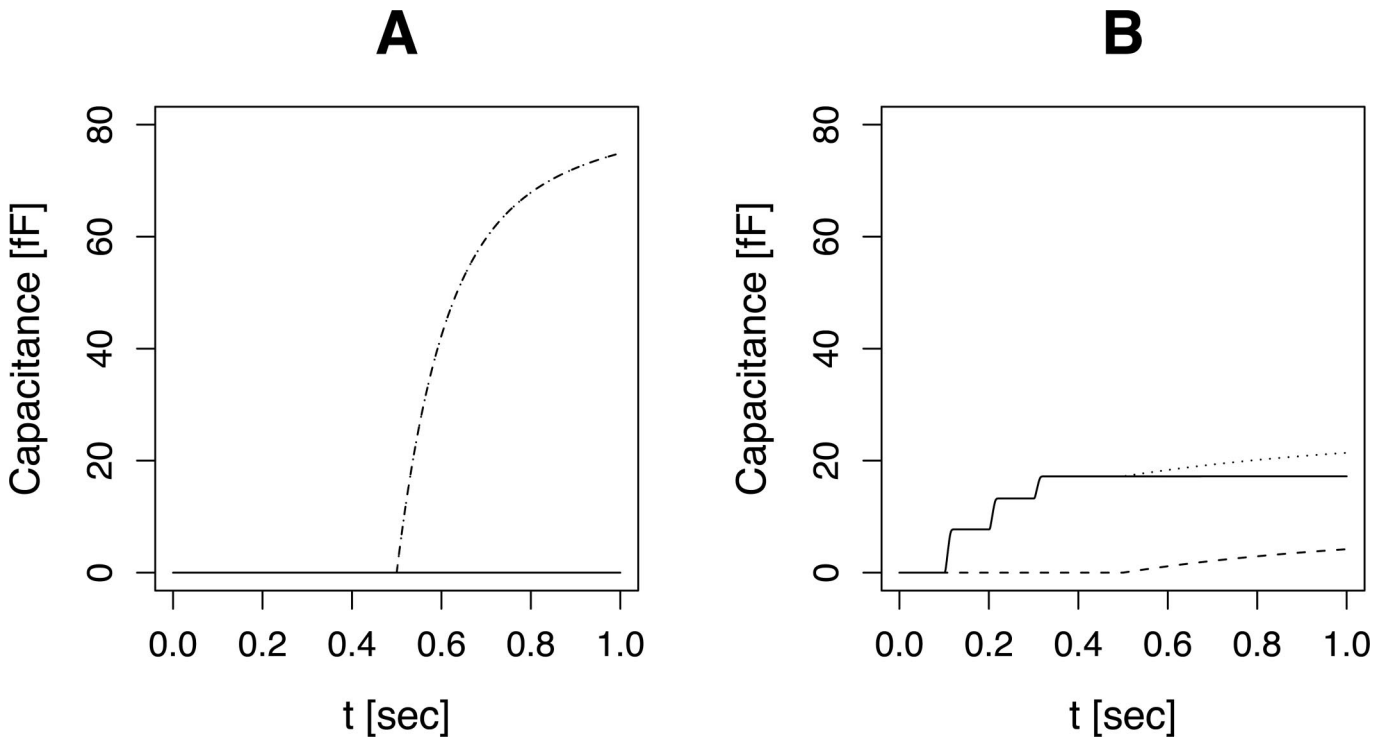

Fig. S4. (*A*) Predicted fast HCSP protocol for Synt-1A knockout (1). Parameters are as in Fig. S3*A*. (*B*) Predicted fast HCSP protocol for hypothetical knockout of HCSP Ca^{2+} sensor. Parameters are as in Fig. S3*B*.

1. Ohara-Imaizumi M, et al. (2007) Imaging analysis reveals mechanistic differences between first- and second-phase insulin exocytosis. *J Cell Biol* 177:695–705.